Arch Appl Mech (2006) 76: 133–144
DOI 10.1007/s00419-006-0010-3

ORIGINAL

Eduardo Lutterbach Bandeira · Marcelo Amorim Savi
Paulo Cesar da Camara Monteiro Jr.
Theodoro Antoun Netto

Finite element analysis of shape memory alloy adaptive trusses with geometrical nonlinearities

Received: 30 August 2005 / Accepted: 12 January 2006 / Published online: 7 March 2006

Abstract This contribution deals with the nonlinear analysis of shape memory alloy (SMA) adaptive trusses employing the finite element method. Geometrical nonlinearities are incorporated into the formulation together with a constitutive model that describes different thermomechanical behaviors of SMA. It has four macroscopic phases (three variants of martensite and an austenitic phase), and considers different material properties for austenitic and martensitic phases together with thermal expansion. An iterative numerical procedure based on the operator split technique is proposed in order to deal with the nonlinearities in the constitutive formulation. This procedure is introduced into ABAQUS as a user material routine. Numerical simulations are carried out illustrating the ability of the developed model to capture the general behavior of shape memory bars. After that, it is analyzed the behavior of some adaptive trusses built with SMA actuators subjected to different thermomechanical loadings.

Keywords Shape memory alloy · Finite element · Abaqus · Numerical simulation

1 Introduction

Shape memory alloys (SMAs) have been found in a great number of applications in different fields of sciences and engineering. Self-actuating fasteners [9,18,19,21], thermally actuator switches and several bioengineering devices are some examples of these applications [15,24,27,28]. Aerospace technology are also using SMAs to solve important problems, in particular those concerning with space savings achieved by self-erectable structures, stabilizing mechanisms, non-explosive release devices and other possibilities [14,31]. Micromanipulators and robotics actuators have been built employing SMAs properties to mimic the smooth motions of human muscles [16,17,37,49]. Moreover, SMAs are being used as actuators for vibration and buckling control of flexible structures [8,35,37].

This contribution proposes a finite element formulation to deal with shape memory bars with geometrical nonlinearities. Finite element modeling of SMA structures has been previously addressed by Brinson and Lammering [12], where a constitutive theory based on Tanaka's model [41,42], and later modified by Brinson [11], has been employed to describe the SMA behavior. Auricchio and Taylor [1] have also proposed a three-dimensional finite element model. Savi et al. [39] discuss an iterative numerical procedure that has been

E. L. Bandeira · M. A. Savi (✉)
Departamento de Engenharia Mecânica, COPPE – Universidade Federal do Rio de Janeiro, 21.941.972,
P.O. Box 68.503, Rio de Janeiro, Brazil
E-mail: eduband@terra.com.br; savi@ufrj.br

P.C. da Camara Monteiro Jr. · T. A. Netto
Departamento de Engenharia Oceânica, COPPE–Universidade Federal do Rio de Janeiro, LTS 21.945.970,
P.O. Box 68.508, Rio de Janeiro, Brazil
E-mail: camara@lts.coppe.ufrj.br; tanetto@lts.coppe.ufrj.br

developed to deal with both geometrical and constitutive nonlinearities in the finite element model for adaptive trusses with SMA actuators. Langoudas et al. [23] consider the thermomechanical response of a laminate with SMA strips where the thermomechanical response is based on Boyd–Lagoudas' polynomial hardening model [10]. Kouzak et al. [20] also treats SMA beams using a constitutive equation proposed by Brinson [11]. Recently, La Cava et al. [22] considers SMA bars with the constitutive model developed by Baêta-Neves et al. [6] exploiting some non-homogeneous situations.

Literature presents other references employing the finite element method (FEM) to analyze the SMA behavior. The response of SMA beams is treated by Collet et al. [13], which analyzes the dynamical response, as well Auricchio and Sacco [2]. Helical springs are modeled with the aid of FEM as can be seen in Toi et al. [44]. Moreover, Wang et al. [48] analyze the effect of crack in phase transformations. SMA composites are recently treated by Auricchio and Petrini [3,4] in three-dimensional medias. A solid finite element is presented to describe the thermo-electro-mechanical problem that is used to simulate different SMA composite applications. Dual kriging interpolation has been employed with FEM in order to describe the shape memory behavior in different reports [45–47]. Masud et al. [29], Bhattacharyya et al. [7], Liu et al. [26] are other contributions in this field.

Here, the FEM is employed promoting the spatial discretization of bars using a constitutive equation proposed by Paiva et al. [33,34] to describe the thermomechanical behavior of SMA trusses. This model includes four macroscopic phases in the formulation: three variants of martensite and an austenitic phase. Furthermore, different material parameters for austenitic and martensitic phases are concerned. The constitutive model captures the general behavior of themomechanical behavior of SMAs providing the description of different phenomena. Geometrical nonlinearities are also included into the formulation. An iterative numerical procedure based on the operator split technique [30] is employed in order to deal with the nonlinearities in the constitutive formulation. This procedure is introduced into ABAQUS as a user material routine. Therefore, Newton method is used together with the orthogonal projection algorithm. Numerical simulations are carried out showing different behaviors of SMA bars. Results show that the finite element model is able to capture the general behavior of SMAs. The analysis of adaptive trusses with SMA actuators subjected to different thermomechanical loadings is carried out showing some interesting behaviors.

2 Mathematical modeling

This section presents the mathematical modeling related to shape memory trusses with geometrical nonlinearities. Basically, a brief introduction is presented to the constitutive model developed by Paiva et al. [33,34] and its coupling with the FEM.

2.1 Constitutive model

There are different ways to describe the thermomechanical behavior of SMAs [32]. Here, a constitutive model presented by Paiva et al. [33,34] is employed [6,38,40]. This model describes different aspects related to the thermomechanical behavior of SMAs, considering different material properties and four macroscopic phases. The model also considers plastic strains and plastic-phase transformation coupling, which turns possible the two-way shape memory effect description. Moreover, tensile–compressive asymmetry is taken into account. The following set of equations is used to describe the thermomechanical behavior of SMA. Notice that, for simplicity, plastic effect is not presented. With these assumptions, the constitutive equations describe the uniaxial stress, σ, as a function of total strain, ε, temperature, T, and three volumetric fractions related to two variants of martensite, β_1 and β_2, and austenite, β_3.

$$\sigma = E\,\varepsilon + \left(\alpha^{\mathrm{C}} + E\alpha_{\mathrm{h}}^{\mathrm{C}}\right)\beta_2 - \left(\alpha^{\mathrm{T}} + E\alpha_{\mathrm{h}}^{\mathrm{T}}\right)\beta_1 - \Omega\,(T - T_0) \tag{1}$$

$$\dot{\beta}_1 = \frac{1}{\eta_1}\Big\{\alpha^{\mathrm{T}}\varepsilon + \Lambda_1 + \left(\alpha_{\mathrm{h}}^{\mathrm{C}}\alpha^{\mathrm{T}} + \alpha_{\mathrm{h}}^{\mathrm{T}}\alpha^{\mathrm{C}} + E\alpha_{\mathrm{h}}^{\mathrm{T}}\alpha_{\mathrm{h}}^{\mathrm{C}}\right)\beta_2 - \left(2\,\alpha_{\mathrm{h}}^{\mathrm{T}}\alpha^{\mathrm{T}} + E\,\alpha^{\mathrm{T_h}2}\right)\beta_1 + \alpha_{\mathrm{h}}^{\mathrm{T}}\left[E\,\varepsilon - \Omega\,(T - T_0)\right] - \partial_1 J_\pi\Big\} + \partial_1 J_\chi \tag{2}$$

$$\dot{\beta}_2 = \frac{1}{\eta_2}\Big\{-\alpha^{\mathrm{C}}\varepsilon + \Lambda_2 + \left(\alpha_{\mathrm{h}}^{\mathrm{T}}\alpha^{\mathrm{C}} + \alpha_{\mathrm{h}}^{\mathrm{C}}\alpha^{\mathrm{T}} + E\alpha_{\mathrm{h}}^{\mathrm{C}}\alpha_{\mathrm{h}}^{\mathrm{T}}\right)\beta_1 - \left(2\,\alpha_{\mathrm{h}}^{\mathrm{C}}\alpha^{\mathrm{C}} + E\,\alpha_{\mathrm{h}}^{\mathrm{C}2}\right)\beta_2 - \alpha_{\mathrm{h}}^{\mathrm{C}}\left[E\,\varepsilon - \Omega\,(T - T_0)\right] - \partial_2 J_\pi\Big\} + \partial_2 J_\chi \tag{3}$$

$$\dot{\beta}_3 = \frac{1}{\eta_3}\left\{-\frac{1}{2}\left(E_{\mathrm{A}} - E_{\mathrm{M}}\right)\left(\varepsilon + \alpha_{\mathrm{h}}^{\mathrm{C}}\beta_2 - \alpha_{\mathrm{h}}^{\mathrm{T}}\beta_1\right)^2 + \Lambda_3 + \left(\Omega_{\mathrm{A}} - \Omega_{\mathrm{M}}\right)\left(T - T_0\right)\right.$$
$$\left.\left(\varepsilon + \alpha_{\mathrm{h}}^{\mathrm{C}}\beta_2 - \alpha_{\mathrm{h}}^{\mathrm{T}}\beta_1\right) - \partial_3 J_\pi\right\} + \partial_3 J_\chi \tag{4}$$

where $E = E_{\mathrm{M}} + \beta_3 \left(E_{\mathrm{A}} - E_{\mathrm{M}}\right)$ is the elastic modulus while $\Omega = \Omega_{\mathrm{M}} + \beta_3 \left(\Omega_A - \Omega_M\right)$ is related to the thermal expansion coefficient. The term T_0 represents a reference temperature where the strain vanishes in a free stress state. Notice that subscript "A" refers to austenitic phase, while "M" refers to martensite. Besides, different properties are assumed to consider tension–compression asymmetry, where the superscript "T" refers to tensile while "C" is related to compressive properties. Hence, $\alpha^{\mathrm{C,T}}$ and $\alpha_{\mathrm{h}}^{\mathrm{C,T}}$ are parameters, respectively associated with the vertical and horizontal sizes of the hysteresis loop. Moreover, parameters Λ_1, Λ_2 and Λ_3 are associated with phase transformations stress levels and are temperature dependent as follows:

$$\Lambda_1 = \frac{L^{\mathrm{T}}}{T_{\mathrm{M}}}(T - T_{\mathrm{M}});\ \Lambda_2 = \frac{L^{\mathrm{C}}}{T_{\mathrm{M}}}(T - T_{\mathrm{M}}) \text{ and } \Lambda_3 = \frac{L^{\mathrm{A}}}{T_{\mathrm{M}}}(T - T_{\mathrm{M}}) \tag{5}$$

where T_{M} is the temperature below which the martensitic phase becomes stable, while L^{T}, L^{C} and L^{A} are parameters related to critical stress for the various phase transformations.

The terms $\partial_n J_\pi$ (n = 1,2,3) corresponds to the sub-differentials of the indicator function J_π with respect to β_n [36]. The indicator function J_π (β_1, β_2, β_3) is related to the convex set π, which provides the internal constraints related to the phases' coexistence. With respect to the evolution equations of volumetric fractions, η_1, η_2 and η_3 represent the internal dissipation related to phase transformations. Moreover $\partial_n J_\chi$ (n = 1,2,3) are the sub-differentials of the indicator function J_χ with respect to $\dot{\beta}_n$ [36]. This indicator function is related to the convex set χ, establishing conditions for the correct description of internal sub-loops due to incomplete phase transformations and also avoids phase transformations of the type: $M + \rightarrow M$ or $M \rightarrow M$ [38].

Besides, in order to consider different phase transformation kinetics for loading and unloading processes, the parameters η_n (n = 1,2,3), related to phase transformation internal dissipation, may assume different values. Therefore, $\eta_n = \eta_n^L$ if $\dot{\varepsilon} > 0$ and $\eta_n = \eta_n^U$ if $\dot{\varepsilon} < 0$.

2.2 Finite element method

In order to present the finite element formulation, consider a SMA bar subjected to a constant axial load. By assuming that ${}_t^{t+\Delta t}\sigma$ is the second Piola–Kirchhoff tensor, ${}_t^{t+\Delta t}\varepsilon$ is the Lagrange strain tensor and ${}^{t+\Delta t}R$ is the work of external forces, all of them evaluated in time instant $t + \Delta t$, the principle of virtual work [5] is given by,

$$\int_{{}^tV} {}_t^{t+\Delta t}\sigma\,\delta\left({}_t^{t+\Delta t}\varepsilon\right)\mathrm{d}^tV = {}^{t+\Delta t}R \tag{6}$$

Notice that $\delta(\ )$ represents a variation of the quantity $(\ )$. The stress tensor can be split into two parts: the increment tensor $\Delta\sigma$, and the stress tensor evaluated in the instant t, ${}_t^t\sigma$. Therefore,

$${}_t^{t+\Delta t}\sigma = {}_t^t\sigma + \Delta\sigma \tag{7}$$

The second Piola–Kirchhoff tensor in the time instant t is the same as the Cauchy stress tensor in this time instant, ${}^t\tau$ Therefore, ${}_t^{t+\Delta t}\sigma = {}^t\tau + \Delta\sigma$.

Since the strain component ${}_t^{t+\Delta t}\varepsilon$ is unknown, it is assumed that this strain tensor is approximated by its increments in the time t, $\Delta\varepsilon$. Moreover, this increment can be split into two terms, associated with the linear and nonlinear part of strain, denoted respectively, by Δe and $\Delta\eta$. Hence,

$$\Delta\varepsilon = \Delta e + \Delta\eta \tag{8}$$

At this point, all these definitions are introduced into the principle of virtual work:

$$\int_{{}^tV} {}^t\tau\,\delta(\Delta e)\mathrm{d}^tV + \int_{{}^tV} {}^t\tau\,\delta(\Delta\eta)\mathrm{d}^tV + \int_{{}^tV} \Delta\sigma\,\delta(\Delta e)\mathrm{d}^tV + \int_{{}^tV} \Delta\sigma\,\delta(\Delta\eta)\mathrm{d}^tV = {}^{t+\Delta t}R \tag{9}$$

Now, for the sake of simplicity, SMA constitutive equation is rewritten as follows:

$$\Delta\sigma = E\Delta\varepsilon + \Delta\Lambda \tag{10}$$

where $\Delta\Lambda = E\left(\alpha_{\mathrm{h}}^{\mathrm{C}}\Delta\beta_2 - \alpha_{\mathrm{h}}^{\mathrm{T}}\Delta\beta_1\right) + \alpha^{\mathrm{C}}\Delta\beta_2 - \alpha^{\mathrm{T}}\Delta\beta_1 - \Omega\Delta(T - T_0)$. Now, using this constitutive equation into the principle of virtual work, it is possible to write:

$$\begin{aligned}
&\int_{{}^tV} {}^t\tau\delta\left(\Delta u_{,x}\right)\mathrm{d}^tV + \int_{{}^tV} {}^t\tau\,\Delta u_{,x}\delta(\Delta u_{,x})\mathrm{d}^tV + \int_{{}^tV} E\Delta u_{,x}\,\delta\left(\Delta u_{,x}\right)\mathrm{d}^tV \\
&+\frac{1}{2}\int_{{}^tV} E(\Delta u_{,x})^3\delta(\Delta u_{,x})\mathrm{d}^tV + \int_{{}^tV} E(\Delta u_{,x})^2\delta(\Delta u_{,x})\mathrm{d}^tV + \frac{1}{2}\int_{{}^tV} E(\Delta u_{,x})^2\delta(\Delta u_{,x})\mathrm{d}^tV \\
&+\int_{{}^tV} \Delta\Lambda\delta(\Delta u_{,x})\mathrm{d}^tV + \int_{{}^tV} \Delta\Lambda\,\Delta u_{,x}\,\delta(\Delta u_{,x})\mathrm{d}^tV = {}^{t+\Delta t}R
\end{aligned} \tag{11}$$

Notice that, $\Delta e = \Delta u_{,x}$ and $\Delta\eta = \frac{(\Delta u_{,x})^2}{2}$, where $(\,)_{,x}$ represents derivation with respect to x. Therefore, neglecting higher order terms, the equation can be written in terms of increments,

$$\begin{aligned}
&\int_{{}^tV} {}^t\tau\delta(\Delta u_{,x})\mathrm{d}^tV + \int_{{}^tV} {}^t\tau\,\Delta u_{,x}\,\delta(\Delta u_{,x})\mathrm{d}^tV + \int_{{}^tV} E\Delta u_{,x}\,\delta(\Delta u_{,x})\mathrm{d}^tV + \int_{{}^tV} \Delta\Lambda\delta(\Delta u_{,x})\mathrm{d}^tV \\
&+\int_{{}^tV} \Delta\Lambda\,\Delta u_{,x}\,\delta(\Delta u_{,x})\mathrm{d}^tV = {}^{t+\Delta t}R.
\end{aligned} \tag{12}$$

The work of external forces can be evaluated by the following equation

$${}^{t+\Delta t}R = \int_{t+\Delta t V} {}^{t+\Delta t}f^{\mathrm{B}}\delta(\Delta u)\mathrm{d}V + \int_{t+\Delta t S} {}^{t+\Delta t}f^{S}\delta(\Delta u)\mathrm{d}S, \tag{13}$$

where ${}^{t+\Delta t}f^{\mathrm{B}}$ are the body forces and ${}^{t+\Delta t}f^{\mathrm{S}}$are the surface forces acting on the bar.

At this point, the continuous function Δu is discretized with the aid of the finite element formulation. Therefore assuming a two-point element, where Lagrange shape functions are considered, one writes a discrete version of the SMA bar governing equation:

$$[K]\{U\} = \{F\} - \{\hat{F}\} \tag{14}$$

where $\{U\}$ are the nodal displacement increment vector, $[K] = [K_{\mathrm{L}}] + [K_{\mathrm{NG}}] + [K_{\mathrm{NC}}]$ is the stiffness matrix. Notice that $[K_{\mathrm{L}}]$ is the linear stiffness matrix and the terms related to geometrical nonlinearities are expressed in $[K_{\mathrm{NG}}]$, while constitutive nonlinearities are expressed in $[K_{\mathrm{NC}}]$. Moreover, $\{F\} = \{R\} - \{F_\tau\}$ is the increment force vector while $\{\hat{F}\} = \{F_\Lambda\}$ is the nonlinear vector force. All these matrixes and vectors are given by:

$$\begin{aligned}
[K_{\mathrm{NG}}] &= \int_{{}^tV} [B]^{\mathrm{T}}\,{}^t\tau_t[B]\mathrm{d}^tV, \quad \{F\} = \int_{{}^tV} [N]^{\mathrm{T}}f^{\mathrm{B}}\mathrm{d}^tV + \int_{{}^tS} [N]^{\mathrm{T}}f^{\mathrm{S}}\mathrm{d}^tS \\
[K_{\mathrm{NC}}] &= \int_{{}^tV} [B]^{\mathrm{T}}\Lambda_t[B]\mathrm{d}^tV, \quad \{F_\tau\} = \int_{{}^tV} [B]^{\mathrm{T}}\,{}^t\tau\,\mathrm{d}^tV \\
[K_{\mathrm{L}}] &= \int_{{}^tV} [B]^{\mathrm{T}}E_t[B]\mathrm{d}^tV, \quad \{F_\Lambda\} = \int_{{}^tV} [B]^{\mathrm{T}}\,{}_t\Lambda\mathrm{d}^tV
\end{aligned} \tag{15}$$

In order to deal with nonlinearities in the formulation, an iterative numerical procedure is employed. In terms of constitutive equations, numerical procedure is explained in Paiva et al. [33,34]. Nevertheless, it is necessary to consider Newton method in order to solve the discrete governing equations.

3 Model verification

The proposed formulation is introduced into ABAQUS as user material procedure. This section presents the model verification through comparisons between the results predicted by the proposed model and experimental data reported in Tobushi et al. [43], which describes tensile tests on Ni–Ti wires at different temperatures. Basically, two different temperatures are considered: 373 K and 353 K. The model parameters identified for this simulation are presented in Table 1, which is used for all numerical simulations of this article [33,34]. Notice that tensile-compressive symmetry is assumed and therefore, $\alpha^{\mathrm{C}} = \alpha^{\mathrm{T}} = \alpha$ and $\alpha_{\mathrm{h}}^{\mathrm{T}} = \alpha_{\mathrm{h}}^{\mathrm{C}} = \alpha_{\mathrm{h}}$. After that, some numerical simulations are performed in order to verify the ability of the proposed model to describe the SMA behavior. Since experimental results are related to a tensile test, it is assumed a homogeneous thermomechanical load process, allowing a comparison between the FEM formulation with experimental results, considering a single constitutive point. A single element is used with this aim, assuming a maximum time step of 5×10^{-3}.

Figure 1 presents a comparison between numerical and experimental results for two different temperatures. Notice that, even though this is a pseudoelastic test, experimental data presents a residual strain at the end of the loading–unloading process, which is probably related to transformation induced plasticity [25,33,34]. However, it should be pointed out the ability of the finite element model to describe the SMA behavior.

Table 1 Model parameters obtained through comparison between numerical and experimental results provided by Tobushi et al. [43] for a Ni–Ti SMA alloy

E_{A} (GPa)	54
E_{M} (GPa)	42
Ω_{A} (MPa/K)	0.74
Ω_{M} (MPa/K)	0.17
α (MPa)	330
L^{T}, L^{C}(MPa)	229
L^{A} (MPa)	44
T_{M} (K)	291.4
T_0 (K)	295
α_h	0.047
η_1^L (MPa.tu)	1
η_1^U (MPa.tu)	2.7
η_3^L (MPa.tu)	1
η_3^U (MPa.tu)	2.7

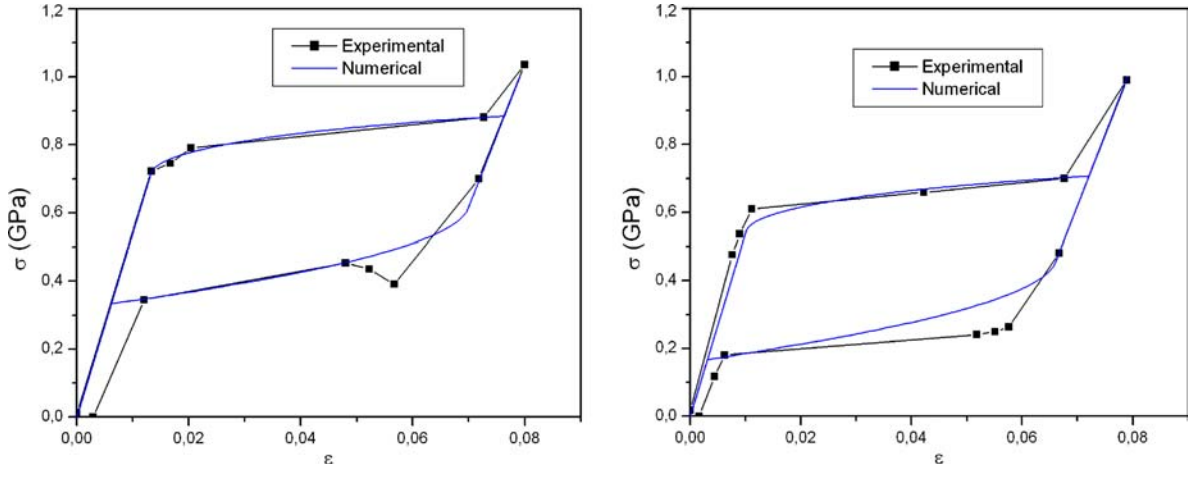

Fig. 1 Model verification

4 Adaptive trusses

In this section, the proposed procedure is applied to analyze some adaptive trusses with shape memory actuators considering three examples. The first one treats a two-bar truss while the second one considers a truss with nine bars. The third example considers a truss structure clearly showing geometric nonlinearities. These examples consider different thermomechanical loadings.

4.1 Two-bar truss

A two-bar truss built by bars with cross-section area 1 cm^2, subjected to thermomechanical loadings presented in Fig. 2, is now considered.

Initially, it is assumed that a single bar is built with SMA ①, while the other one is a typical steel ② ($E = 200$ GPa, $\nu = 0.3$). Figure 3 shows deformed configuration compared with the initial one for two different time instants: the first is related to the end of the mechanical process while the second is associated with the end of thermal loading. The displacements are shown in real scale and their vertical values must be seen in Fig. 4. Notice that the thermal loading changes the position of the truss, although the mechanical loading is not removed.

Figure 4 shows the vertical displacement related to the node where the force is applied and also the stress–strain curve. Again it is possible to see the movement of the bar caused by the temperature variation. It is noticeable that geometrical nonlinearities introduce some characteristics of the response as the non-horizontal curve of the stress–strain relation in the region related to the thermal loading.

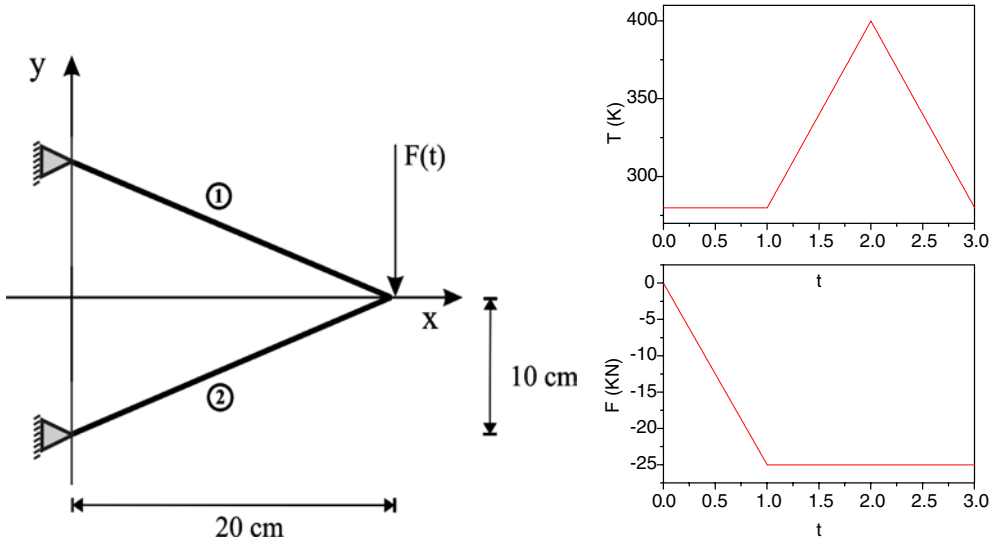

Fig. 2 Two-bar truss

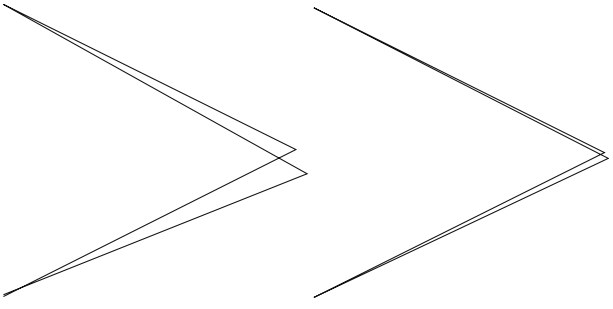

Fig. 3 Comparison between deformed and initial configurations of the two-bar truss

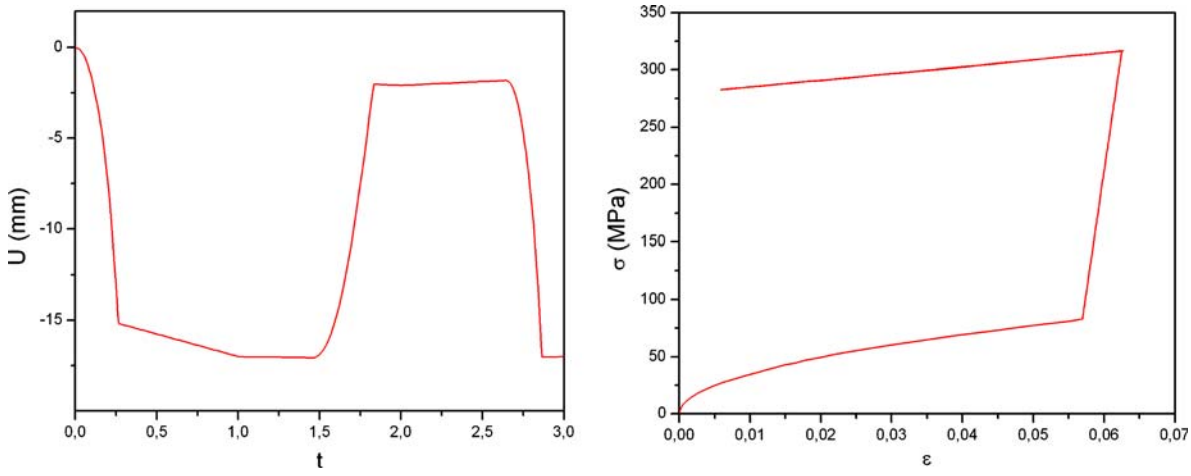

Fig. 4 Displacement time history and stress–strain curve

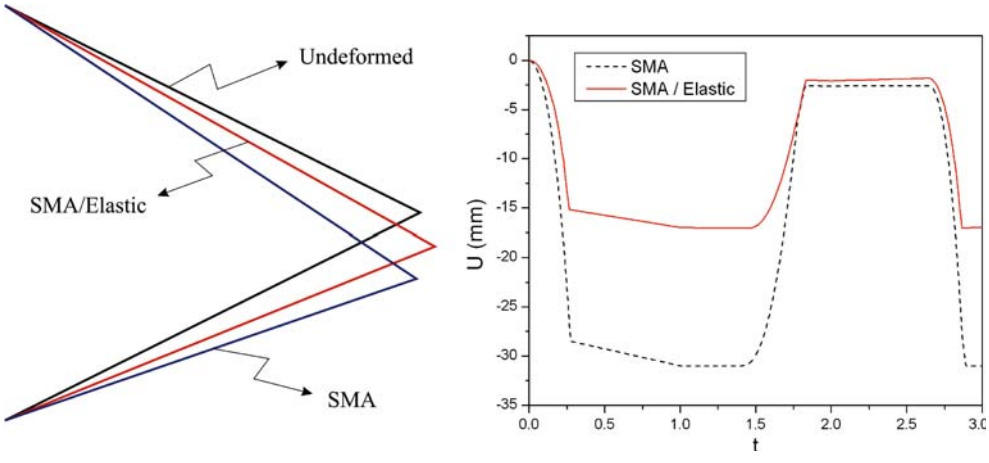

Fig. 5 Two-bar truss with two SMA bars

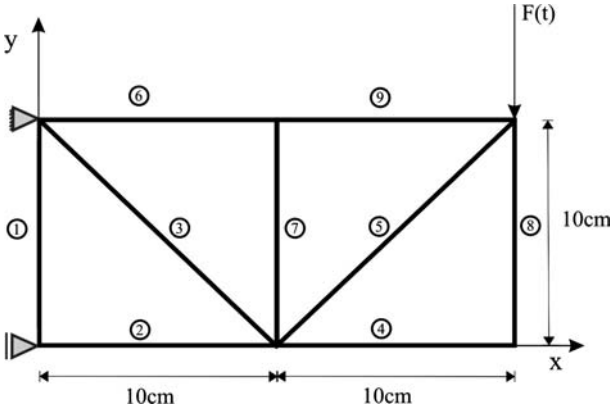

Fig. 6 Nine-bar truss

At this point, it is assumed that both truss bars are built with SMA. This new truss has smaller stiffness presenting greater displacements. Figure 5 compares results of both problems showing that SMA can also recover displacements even though mechanical force is not removed.

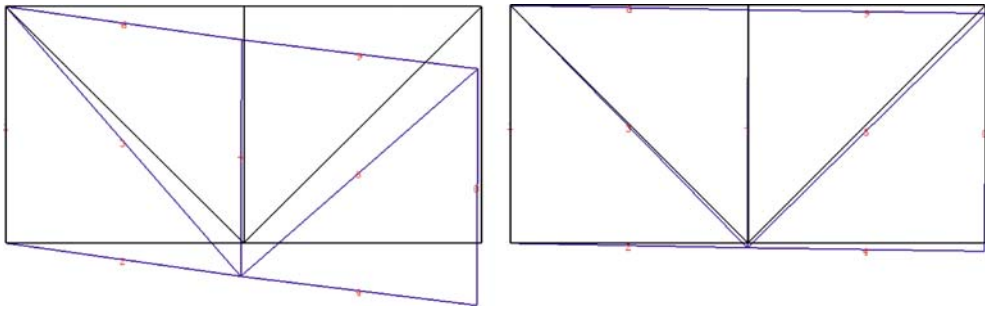

Fig. 7 Comparison between deformed and initial configurations of the nine-bar truss

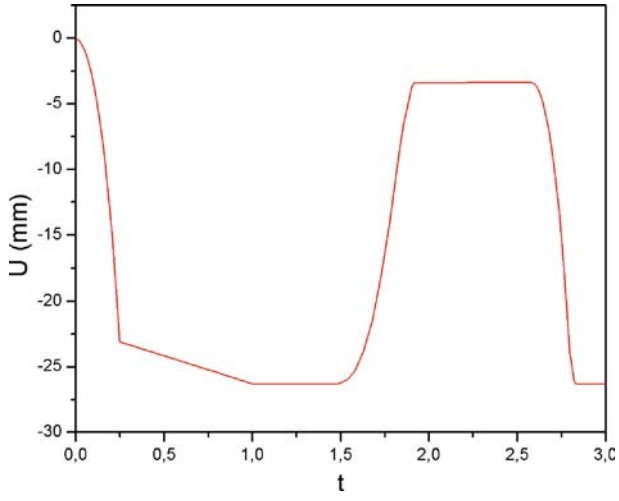

Fig. 8 Time history of displacements

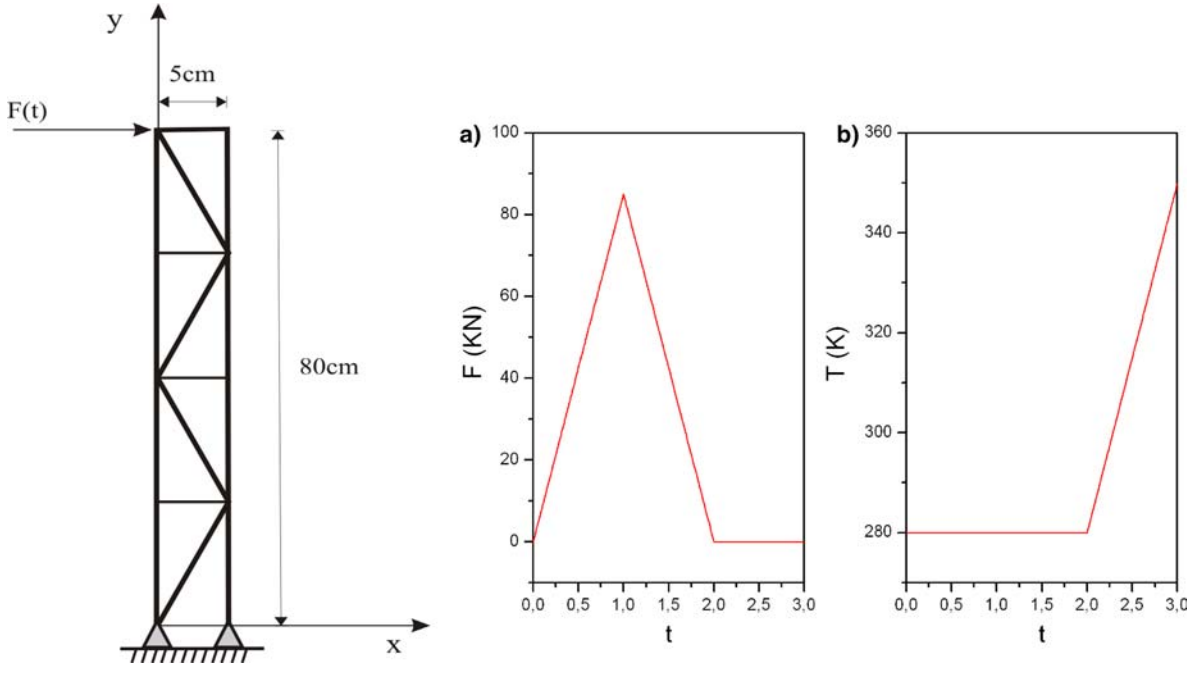

Fig. 9 Adaptive truss built with shape memory alloy bars

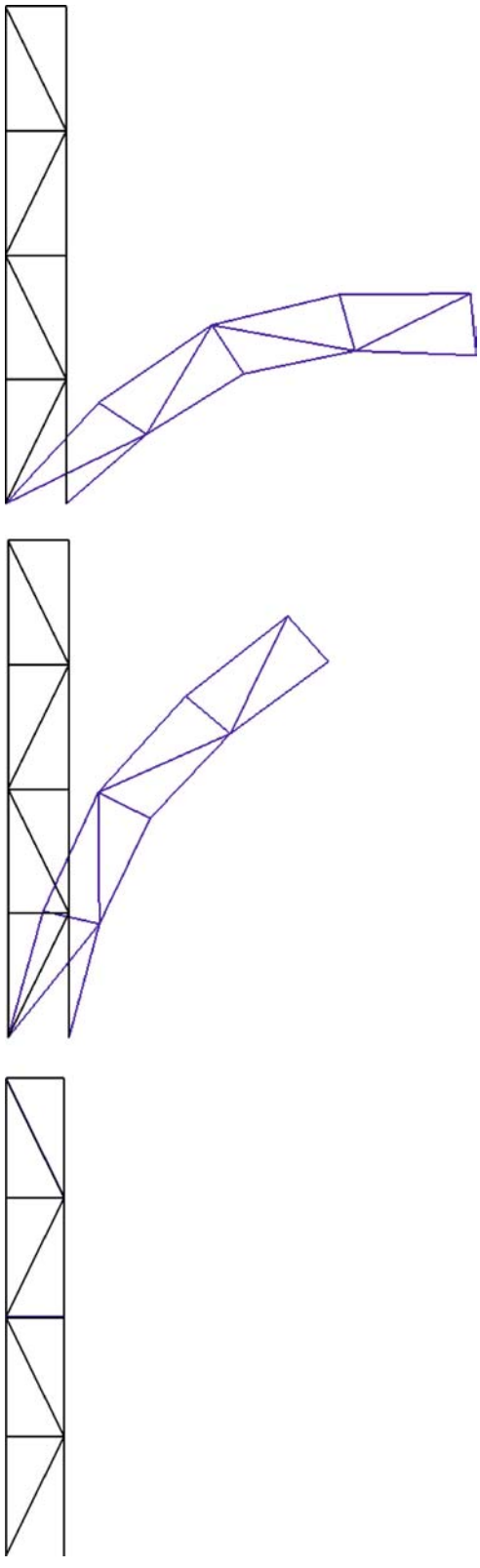

Fig. 10 Adaptive truss response in different time instants

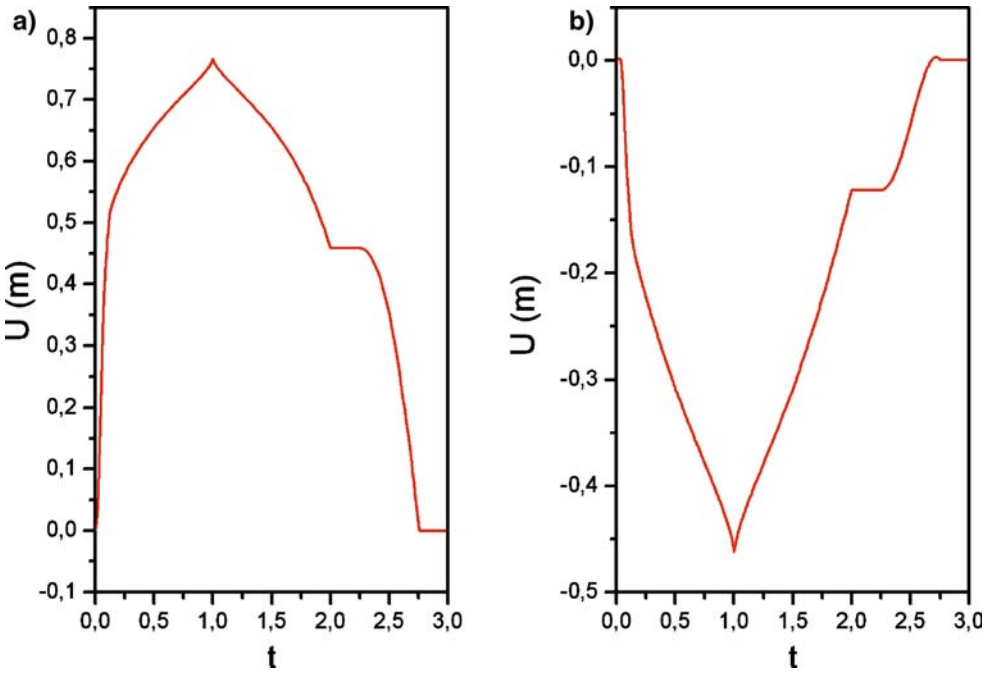

Fig. 11 **a** Horizontal displacement. **b** Vertical displacement

4.2 Nine-bar truss

At this point, a nine-bar truss is treated considering that each bar has a cross-section area of 1 cm^2 (Fig. 6), subjected to a thermomechanical loading presented in Fig. 3. Bars 3 and 5 are built with SMA, while the others are constructed with typical steel ($E = 200$ GPa, $\nu = 0.3$). With this assumption, the SMA bars represent discrete actuators of this structure.

Figure 7 shows deformed configuration compared with the initial one for two different time instants: the first is related to the end of the mechanical process while the second is associated with the end of thermal loading. Notice that, again, the thermal loading changes the truss position, although the mechanical loading is not removed. This behavior is clearly observed in the time history of displacements. Figure 8 shows the vertical displacement related to the node where the force is applied, showing the truss movement caused by the temperature variation.

4.3 Truss structure

An adaptive truss built with 16 SMA bars is now focused on. Each bar has a cross-section area of 1 cm^2. Figure 9 shows a schematic picture of the structure together with the thermomechanical loading process related to a shape memory effect. Basically, the mechanical loading is applied when the structure is at $T = 280$ K ($T < T_M$). Since this structure presents large displacements, it is assumed that force follows the application node. When the mechanical loading is finished, a temperature variation is imposed to the structure.

Figure 10 shows different configurations of the structure response for the cited thermomechanical loading, considering different time instants. The first picture shows the time instant related to the maximum value of the mechanical loading. Notice the large displacements and rotations associated with this configuration. The second picture presents the time instant when the mechanical loading is completed removed. Under this condition, the system present a residual strain related to the martensitic phase. Finally, the last picture presents the time instant after the temperature increasing. At this point, the structure eliminates all residual strains. Figure 11 presents both horizontal and vertical displacement time history related to the node where the force is applied. Notice linear regions associated with elastic response and also nonlinear regions related to the phase transformation response.

5 Conclusions

This article presents a nonlinear finite element analysis of shape memory adaptive trusses. A constitutive model proposed by Paiva et al. [33,34] is used to describe the thermomechanical behavior of SMAs. FEM is used to perform spatial discretization allowing the analysis of non-homogeneous problems. Geometrical nonlinearities are incorporated into the formulation. An iterative numerical procedure based on the operator split technique is employed in order to deal with constitutive nonlinearities. This procedure is introduced into ABAQUS as a user material routine and, therefore, Newton method is used together with this orthogonal projection algorithm. Numerical simulations show that results from FEM capture the SMA general behavior. Moreover, other simulations show the response of adaptive truss built with SMA actuators. The capability of the proposed formulation to describe SMA adaptive truss may be exploited in different applications, becoming an important tool for design purposes.

Acknowledgements The authors would like to acknowledge the support of the Brazilian Research Council (CNPq).

References

1. Auricchio, F., Taylor, R.L.: Shape memory alloy superelastic behavior: 3D finite element simulations. In: Proceedings of the 3rd international conference on intelligent materials, Lyon, 3–5, June, (1996)
2. Auricchio, F., Sacco, E.: A temperature- dependent beam for shape memory alloys: Constitutive modeling, finite-element implementation and numerical simulations. Comput Methods Appl Mech Eng **174**, 171–190 (1999)
3. Auricchio, F., Petrini, L.: A three-dimensional model describing stress–temperature induced solid phase transformations: Thermomechanical coupling and hybrid composite applications. Int J Numer Methods Eng **61**(5), 716–737 (2004a)
4. Auricchio, F., Petrini, L.: A three-dimensional model describing stress–temperature induced solid phase transformations: solution algorithm and boundary value problems. Int J Numer Methods Eng **61**(6), 807–836 (2004b)
5. Bathe, K.-J.: Finite element procedures in engineering analysis. Englewood Cliffs: Prentice Hall (1982)
6. Baêta-Neves, A.P., Savi, M.A., Pacheco, P.M.C.L.: On the Fremond's constitutive model for shape memory alloys. Mech Res Commun **31**(6), 677–688 (2004)
7. Bhattacharyya, A., Faulkner, M.G., Amalraj, J.J.: Finite element modeling of cyclic thermal response of shape memory alloy wires with variable material properties. Comput Mater Sci **17**, 93–104 (2000)
8. Birman, V.: Theory and comparison of the effect of composite and shape memory alloy stiffeners on stability of composite shells and plates. Int J Mech Sci **39**(10), 1139–1149 (1997)
9. Borden, T.: Shape memory alloys: forming a tight fit. Mech Eng **113**(10), 66–72 (1991)
10. Boyd, J.G., Lagoudas, D.C.: A thermodynamic constitutive model for the shape memory materials, part I: the monolithic shape memory alloys. Int J Plast **12**(86), 805–842 (1996)
11. Brinson, L.C.: One-dimensional constitutive behavior of shape memory alloys: Termomechanical derivation with non-constant material functions and redefined martensite internal variable. J Intell Mater Syst Struct **4**, 229–242 (1993)
12. Brinson, L.C., Lammering, R.: Finite element analysis of the behavior of shape memory alloys and their applications. Int J Solids Struct **30**(23), 3261–3280 (1993)
13. Collet, M., Foltête, E., Lexcellent, C.: Analysis of the behavior of a shape memory alloy beam under dynamical loading. Eur J Mech A Solids, **20**(4), 615–630 (2001)
14. Denoyer, K.K., Erwin, R.S., Ninneman, R.R.: Advanced smart structures flight experiments for precision spacecraft. Acta Astronaut **47**, 389–397 (2000)
15. Duerig, T.M., Pelton, A., Stöckel, D.: An overview of nitinol medical applications. Mater Sci Eng A **273–275**, 149–160 (1999)
16. Fujita, H., Toshiyoshi, H.: Micro actuators and their applications. Microelectron J **29**, 637–640 (1998)
17. Garner, L.J., Wilson, L.N., Lagoudas, D.C., Rediniotis, O.K.: Development of a shape memory alloy actuated biomimetic vehicle. Smart Mater Struct **9**(5), 673–683 (2001)
18. van Humbeeck, J.: Non-medical applications of shape memory alloys. Mater Sci Eng A **273–275**, 134–148 (1999)
19. Kibirkstis, E., Liaudinskas, R., Pauliukaitis, D., Vaitasius, K.: Mechanisms with shape memory alloy. J Phys IV, **C5**, 633–636 (1997)
20. Kouzak, Z., Levy Neto, F., Savi, M.A.: Finite element model for composite beams using SMA fibers. In: Proceedings of CEM NNE 98 – V Congresso de Engenharia Mecânica Norte e Nordeste, vol **II**, Fortaleza, Brazil, 27–30 October, pp 112–119 (1998)
21. La Cava, C.A.P.L., Silva, E.P., Machado, L.G., Pacheco, P.M.C.L., Savi, M.A.: Modeling of a shape memory preload device for bolted joints. In: Proceedings of CONEM 2000 – Congresso Nacional de Engenharia Mecânica, Natal, Brazil (in portuguese) (2000)
22. La Cava, C.A.P.L., Savi, M.A., Pacheco, P.M.C.L.: A nonlinear finite element method applied to shape memory bars. Smart Mater Struct **13**(5), 1118–1130 (2004)
23. Lagoudas, D.C., Moorthy, D., Qidwai, M.A., Reddy, J.N.: Modeling of the thermomechanical response of active laminates with SMA strips using the layerwise finite element method. J Intell Mater Syst Struct **8**, 476–488 (1997)
24. Lagoudas, D.C., Rediniotis, O.K., Khan, M.M.: Applications of shape memory alloys to bioengineering and biomedical technology. In: Proceedings of 4th international workshop on mathematical methods in scattering theory and biomedical technology, October 1999, Perdika, Greece (1999)

25. Lagoudas, D.C., Entchev, P.B., Kumar, P.K.: Thermomechanical characterization SMA actuators under cyclic loading. In: Proceedings of IMECE'03, 2003 ASME international mechanical engineering congress, Washington, 15–21, November (2003)
26. Liu, K.M., Kitipornchai, Ng, T.Y., Zou, G.P.: Multi-dimensional superelastic behavior of shape memory alloys via nonlinear finite element method. Eng Struct **24**, 51–57 (2002)
27. Machado, L.G., Savi, M.A.: Odontological applications of shape memory alloys. Rev Bras Odontol **59**(5), 302–306 (in portuguese) (2002)
28. Machado, L.G., Savi, M.A.: Medical applications of shape memory alloys. Braz J Med Biol Res **36**(6), 683–691 (2003)
29. Masud, A., Panahandeh, M., Aurrichio, F.: A finite-strain finite element model for the pseudoelastic behavior of shape memory alloys. Comput Methods Appl Mech Eng **148**, 23–37 (1997)
30. Ortiz, M., Pinsky, P.M., Taylor, R.L.: Operator split methods for the numerical solution of the elastoplastic dynamic problem. Comput Methods Appl Mech Eng **39**, 137–157 (1983)
31. Pacheco, P.M.C.L., Savi, M.A.: A non-explosive release device for aerospace applications using shape memory alloys. In: Proceedings of XIV Congresso Brasileiro de Engenharia Mecânica (COBEM 97 − ABCM), Bauru, Brazil, November (1997)
32. Paiva, A., Savi, M.A.: An overview of constitutive models for shape memory alloys. Math Probl Eng (in press, 2006)
33. Paiva, A., Savi, M.A., Pacheco, P.M.C.L.: Modeling transformation induced plasticity in shape memory alloys. In: Procedings of 18th international congress of mechanical engineering (COBEM 2005 – ABCM), Ouro Preto, Brazil (2005)
34. Paiva, A., Savi, M.A., Braga, A.M.B., Pacheco, P.M.C.L.: A constitutive model for shape memory alloys considering tensile-compressive asymmetry and plasticity. Int J Solids Struct **42**(11,12), 3439–3457 (2005)
35. Pietrzakowski, M.: Natural frequency modification of thermally activated composite plates. Mec Ind **1**, 313–320 (2000)
36. Rockafellar, R.T.: Convex analysis. Princeton: Princeton Press (1970)
37. Rogers, C.A.: Intelligent materials. Sci Am, **273**, 122–127 (1995)
38. Savi, M.A., Paiva, A.: Describing internal subloops due to incomplete phase transformations in shape memory alloys. Arch Appl Mech **74**(9), 637–647 (2005)
39. Savi, M.A., Braga, A.M.B., Alves, J.A.P., Almeida, C.A.: Finite element model for trusses with shape memory alloy actuators. In: Proceedings of EUROMECH 373 colloquium - modeling and control of adaptive mechanical structures, Magdeburg, 11–13 March (1998)
40. Savi, M.A., Paiva, A., Baêta-Neves, A.P., Pacheco, P.M.C.L.: Phenomenological modeling and numerical simulation of shape memory alloys: a thermo-plastic-phase transformation coupled model. J Intell Mater Syst Struct **13**(5), 261–273 (2002)
41. Tanaka, K.: A thermomechanical sketch of shape memory effect: One-dimensional tensile behavior. Res Mech **18**, 251–263 (1986)
42. Tanaka, K., Nagaki, S.: Thermomechanical description of materials with internal variables in the process of phase transformation. Ing Arch **51**, 287–299 (1982)
43. Tobushi, H., Iwanaga, N., Tanaka, K., Hori, T., Sawada, T.: Deformation behavior of Ni-Ti shape memory alloy subjected to variable stress and temperature. Continuum Mech Thermodyn **3**, 79–93 (1991)
44. Toi, Y., Lee, J., Taya, M.: Finite element analysis of superelastic, large deformation behavior of shape memory alloy helical springs. Comput Struct **82**, 1685–1693 (2004)
45. Trochu, F., Qian, Y-Y.: Nonlinear finite element simulation of superelastic shape memory alloy parts. Comput Struct **62**(5), 799–810 (1997)
46. Trochu, F., Terriault, P.: Nonlinear modelling of hystereitc material laws by dual kriging and application. Comput Methods Appl Mech Eng **151**, 545–558 (1998)
47. Trochu, F., SacéPé, N., Volkov, O., Turenne, S.: Characterization of NiTi shape memory alloys using dual kriging interpolation. Mater Sci Eng A **273–275**, 95–399 (1999)
48. Wang, X.M., Wang, Y.F., Baruj, A., Eggeler., Yue, Z.F.: On the formation of martensite in front of cracks in pseudoelastic shape memory alloys. Mater Sci Eng A **394**, 393–398 (2005)
49. Webb, G., Wilson, L., Lagoudas, D.C., Rediniotis, O.: Adaptive control of shape memory alloy actuators for underwater biomimetic applications. AIAA J **38**(2), 325–334 (2000)